SPANDIDOS PUBLICATIONS

INTERNATIONAL JOURNAL OF ONCOLOGY 54: 2127-2138, 2019

C-mannosylation of R-spondin2 activates Wnt/β-catenin signaling and migration activity in human tumor cells

HAYATO MIZUTA[1], KENTA KUGA[1], TAKEHIRO SUZUKI[2], YUKI NIWA[1], NAOSHI DOHMAE[2] and SIRO SIMIZU[1]

[1]Department of Applied Chemistry, Faculty of Science and Technology, Keio University, Yokohama, Kanagawa 223-8522; [2]Biomolecular Characterization Unit, RIKEN Center for Sustainable Resource Science, Wako, Saitama, 351-0198, Japan

Received November 5, 2018; Accepted February 22, 2019

DOI: 10.3892/ijo.2019.4767

Abstract. R-spondin2 (Rspo2), one of the four members of the R-spondin family of proteins, has agonistic activity in the Wnt/β-catenin signaling pathway, and it is associated with normal development, as well as disease, such as cancer. The present study focused on the *C*-mannosylation of Rspo2, which is a novel and unique type of glycosylation that occurs via a C-C linkage between the tryptophan residue and an α-mannose. Although Rspo2 has two putative *C*-mannosylation sites at residues Trp^{150} and Trp^{153}, it had not been reported to date whether these sites are *C*-mannosylated. Firstly, results from mass spectrometry demonstrated that Rspo2 was *C*-mannosylated at the Trp^{150} and Trp^{153} residues. Notably, while this *C*-mannosylation of Rspo2 resulted in increased extracellular secretion in human fibrosarcoma HT1080 cells, in other human tumor cell lines it inhibited secretion. However, *C*-mannosylation had consistent effects on the activation of Wnt/β-catenin signaling in PANC1 and MDA-MB-231 cells, as well as HT1080 cells. Furthermore, overexpression of wild-type Rspo2 significantly increased the migratory ability of A549 and HT1080 cells, whereas overexpression of a *C*-mannosylation-defective mutant enhanced migration to a lesser degree. These results suggested that *C*-mannosylation of Rspo2 may promote cancer progression and that the inhibition of *C*-mannosylation may serve as a potential novel therapeutic approach for cancer therapy.

Correspondence to: Professor Siro Simizu, Department of Applied Chemistry, Faculty of Science and Technology, Keio University, 3-14-1 Hiyoshi, Kohoku-ku, Yokohama, Kanagawa 223-8522, Japan
E-mail: simizu@applc.keio.ac.jp

Abbreviations: CBB, coomassie brilliant blue; DMEM, Dulbecco's modified Eagle's medium; ER, endoplasmic reticulum; LGR, leucine-rich repeat containing G protein-coupled receptor; Ni-NTA, Ni-nitrilotriacetic acid; PBS, phosphate-buffered saline; RNF43, ring finger 43; Rspo2, R-spondin2; TSR1, thrombospondin type 1 repeat; ZNRF3, zinc and ring finger 3

Key words: cell migration, *C*-mannosylation, intracellular trafficking, R-spondin2, Wnt/β-catenin signaling

Introduction

R-spondins consist of a signal peptide, furin repeats and a thrombospondin type 1 repeat (TSR1) domain (1-4). They enhance Wnt/β-catenin signaling by acting as ligands of leucine-rich repeat-containing G protein-coupled receptor (LGR) 4-6, E3 ubiquitin ligase zinc and ring finger 3 (ZNRF3), and its homolog, ring finger 43 (RNF43) (2,5-8). Wnt/β-catenin signaling regulates several developmental events, including embryo morphogenesis, formation of muscle, and limb patterning (9-12). Conversely, Wnt/β-catenin signaling is associated with various diseases, including cancer; thus, abnormal Wnt/β-catenin signaling contributes to tumor cell progression *in vivo* and *in vitro* (9,13).

R-spondin2 (Rspo2), a member of the R-spondin family of proteins, has crucial functions in development through the Wnt/β-catenin signaling pathway. Rspo2 is essential for normal laryngeal-tracheal, lung, and limb morphogenesis, and Rspo2 deficiency results in immediate death following birth (14,15). Additionally, Rspo2 is important for cell differentiation and has been demonstrated to have a role in the mineralization of osteoblasts in osteoarthritis (16), myogenic differentiation, and hypertrophic myotube formation (17). Notably, Rspo2 is also involved in cancer progression. There are two contrasting aspects regarding the function of Rspo2 in cancer progression: It has suppressive activity in colorectal cancer, but promoting in hepatocellular carcinoma and pancreatic cancer (18-20). However, both these opposite functions are regulated by Wnt/β-catenin signaling. Therefore, it is important to examine the association between Wnt/β-catenin signaling and Rspo2 in various types of cancer.

C-mannosylation is a protein modification in which an α-mannose attaches to the indole C2 carbon of the first tryptophan residue of the consensus sequence Trp-Xaa-Xaa-Trp/Cys, via a C-C linkage (21,22). This unique type of glycosylation was first identified in human ribonuclease 2 (23). *C*-mannosylated substrates have been reported for ~25 proteins (24), and have been demonstrated to occur in various mammalian cells, including human, monkey, pig, mouse and hamster (25). The majority of *C*-mannosylated proteins contain the TSR1 domain (26) or are type 1 cytokine receptors that contain a Trp-Ser-Xaa-Trp-Ser motif (27,28). *C*-mannosylation affects protein secretion, intracellular localization, protein folding,

and protein-protein interactions, similar to other forms of glycosylations (29-32); however, the association between disease and *C*-mannosylation is not fully understood. *C*-mannosyltransferase dpy-19 (DPY19) was first identified quite recently as a *C*-mannosyltransferase in *Caenorhabditis elegans* (33). Four homologs of DPY19 exist in mammals, and human dpy-19 like *C*-mannosyltransferase (DPY19L) 3 and mouse DPY19L1 and DPY19L3 have been identified as mammalian *C*-mannosyltransferases (30,34). We previously reported that both Rspo1 and Rspo3 are *C*-mannosylated at two conserved Trp residues (30,35). Although these modifications regulate secretion and Wnt/β-catenin signaling activity in HT1080 cells, the association between tumorigenesis and *C*-mannosylation is not yet fully understood. Furthermore, among the R-spondin family proteins, only Rspo2 has been reported to have a suppressive effect on frizzled class receptor 7 (Fzd7) levels, resulting in a reduction in colorectal cancer cell migration (36). Thus, it is important to investigate the role of Rspo2 in additional tumor cell lines. In the present study, several types of malignant tumor cell lines were used in order to elucidate the role of *C*-mannosylation on Rspo2 function in cancer. These included the pancreatic cancer PANC1 cells, in which Rspo2 acts as an enhancer, as well as the breast cancer MDA-MB-231, lung cancer A549 and fibrosarcoma HT1080 cells.

The current study examined whether Rspo2 was *C*-mannosylated. Using liquid chromatography-tandem mass spectrometry (LC-MS/MS) analysis, Rspo2 was determined to be *C*-mannosylated at Trp^{150} and Trp^{153}, and these modifications were demonstrated to alter its secretory levels and intracellular trafficking. In addition, *C*-mannosylation of Rspo2 regulated the agonistic activity of Rspo2 in the Wnt/β-catenin signaling pathway and on cancer cell migration. The present data indicated that the *C*-mannosylation of Rspo2 may serve as a potential novel therapeutic target for cancer.

Materials and methods

Cell culture. HT1080 human fibrosarcoma (Japanese Collection of Research Bioresources Cell Bank, Osaka, Japan), 293T (RIKEN BioResource Center, Tsukuba, Japan), A549 human lung adenocarcinoma (RIKEN BioResource Center) (37-40), PANC1 human pancreatic adenocarcinoma (RIKEN BioResource Center) and MDA-MB-231 human breast adenocarcinoma cell lines, which was gifted by Professor Masakazu Toi (Kyoto University Graduate School of Medicine, Kyoto, Japan), were all cultured in Dulbecco's modified Eagle's medium (DMEM; Nissui Pharmaceutical Co., Ltd, Tokyo, Japan) supplemented with 6% (v/v) fetal bovine serum (Cosmo Bio Co. Ltd., Tokyo, Japan), 100 U/ml penicillin G, 100 mg/l kanamycin, 600 mg/l L-glutamine, and 2.25 g/l $NaHCO_3$ at 37˚C in a humidified incubator with 5% CO_2. The LoVo human colon adenocarcinoma cell line was cultured in RPMI-1640 medium (Nissui Pharmaceutical Co., Ltd) supplemented with 10% (v/v) fetal bovine serum, 105 U/ml penicillin G, 105 mg/l kanamycin, 314 mg/l L-glutamine, and 2.25 g/l $NaHCO_3$ at 37˚C in a humidified incubator with 5% CO_2.

Plasmid construction. Total RNA was extracted from THP1 cells using RNA extraction buffer (38% (w/w) Phenol, 0.8 M guanidine thiocyanate, 0.4 M ammonium thiocyanate, 0.1 M sodium acetate, 5% (v/v) glycerol), and cDNA was prepared from 2 μg of total RNA with the High-Capacity cDNA Reverse Transcription kit (Applied Biosystems; Thermo Fisher Scientific, Inc.). The resulting cDNA was used for polymerase chain reaction (PCR) amplification with PrimeSTAR Max DNA Polymerase (Takara Bio Inc., Shiga, Japan). The sequences of the primers used to amplify the human Rspo2 cDNA, were: 5'-GAACCCTCCAGTTCCTAGACTTTGA GAGGCGTCTC-3' (forward) and 5'-ATTGGTTAGCTCTGT CTGTAGCTAGGAAGACGCTG-3' (reverse). PCR was performed for 35 cycles with an annealing temperature of 60˚C. The PCR product contained a 5' untranslated region (UTR), the coding sequence for the Rspo2 gene, and a 3'UTR. To obtain the coding region of the Rspo2 gene, a second PCR was performed with the same reagents/conditions as the first PCR, and using the following primers: 5'-TTTTCTCGAGAT GCAGTTTCGCCTTTTCTCCTTTG-3' (forward) and 5'-TTT TGCGGCCGCTTGGTTAGCTCTGTCTGTAGC-3' (reverse). The obtained cDNA was subcloned into pCI-neo (Promega Corporation, Madison, WI, USA) and CSII-CMV-MCS-IRES2-Bsd vectors (RIKEN BioResource Center). To introduce the C-terminal myc-his6 tag, PCR was performed with primers that had Myc and his6 codons. The sequences of the tags were as follows: Myc, 5'-GAACAA AAACTCATCTCAGAAGAGGATCTG-3'; and his6, 5'-CAT CATCACCATCACCAT-3'. Certain tryptophan residues in Rspo2 were substituted with alanine residues by PCR site-directed mutagenesis using the overlap extension technique with PrimeSTAR Max DNA Polymerase. The sequences of primers that were used for the mutagenesis, the number of cycles, and the annealing temperatures were as follows: W150A, 5'-GTGAAGTTGGTCATGCGAGCGAATGGG GAA-3' (forward) and 5'-GTTCCCCATTCGCTCGCATGA CCAACTTCA-3' (reverse), 35 cycles, 63˚C; and W153A, 5'-GAGCGAAGCGGGAACTTG-3' (forward) and 5'-CAA GTTCCCGCTTCGCTC-3' (reverse), 35 cycles, 63˚C. The resulting cDNAs were cloned into the *Xho*I/*Not*I restriction sites of pCI-neo and CSII-CMV-MCS-IRES2-Bsd vectors for mammalian cell expression.

Green fluorescent protein (GFP) cDNA was amplified from pAcGFP1-N1 (Takara Bio Inc.) with PrimeSTAR Max DNA Polymerase and subcloned into CSII-CMV-MCS-IRES2-Bsd. The sequences of the gene-specific primers, the number of cycles, and the annealing temperature were as follows: 5'-TT TTCTCGAGATGGTGAGCAAGGGCGCCGAGCTG-3' (forward) and 5'-TTTTGCGGCCGCTCACTTGTACAGCTC ATCCATGC-3' (reverse), 35 cycles, 63˚C. The resulting cDNA was cloned into the *Xho*I/*Not*I restriction sites of CSII-CMV-MCS-IRES2-Bsd for mammalian cell expression.

Establishment of Rspo2-overexpressing cell lines. HT1080 cells were grown in a 6-well plate at 50-60% confluence and transfected with 2 μg pCI-neo vectors using the Lipofectamine 3000 transfection kit (Thermo Fisher Scientific, Inc.), according to the manufacturer's protocol, in order to establish stable cell lines that expressed wild-type or mutant Rspo2-myc-his6. At 72 h post-transfection, cells were treated with 400 μg/ml G418 (Wako Pure Chemical Industries, Ltd., Osaka, Japan) for selection of stable cells. Clonal cells that

expressed high levels of myc-his6-tagged wild-type and double mutant W150A/W153A (termed herein 2WA) Rspo2 were designated HT1080-Rspo2-MH and HT1080-Rspo2/2WA-MH cells, respectively. Mixed population of W150A-expressing cells were designated HT1080-Rspo2/W150A-MH. Cells that were transfected with the empty pCI-neo vector were termed HT1080-neo (41).

To establish Rspo2-overexpressing A549, PANC1, MDA-MB-231, and LoVo cell lines, the CSII-CMV-MCS-IRES2-Bsd plasmids were transfected into 293T cells using a Lentivirus High Titer Packaging Mix (Takara Bio Inc.) for lentivirus production. After 6 h of transfection, the cells were washed, and fresh medium was added. After an additional 48 h of culture, the conditioned media, containing lentivirus, were collected, and each cell line was infected with the lentivirus media. Following infection, A549, PANC1, MDA-MB-231 and LoVo cells were selected with 20, 10, 7.5 and 15 μg/ml Blasticidin S (Wako Pure Chemical Industries, Ltd.), respectively. Cells that expressed high levels of myc-his6-tagged wild-type and 2WA mutant Rspo2, and GFP which was used for control expression, were used for experiments. Rspo2-overexpressing A549 cells were followed by limiting dilution method to establish clonal cells.

Western blotting. For the western blot analysis, a slightly modified version of a previously described method was used (42-44). Cells were cultured, and then lysed in buffer (50 mM Tris-HCl pH 7.5, 150 mM NaCl, 0.1% SDS, 1% Triton X-100, 1% sodium deoxycholate, and 1 mM PMSF) at 4˚C with sonication. The lysates were centrifuged at 15,300 x g for 10 min, and the amount of protein in each lysate was measured by Coomassie Brilliant Blue (CBB) G-250 staining (Bio-Rad Laboratories, Inc., Hercules, CA, USA). Loading buffer (350 mM Tris-HCl pH 6.8, 30% glycerol, 0.012% bromophenol blue, 6% SDS, and 30% 2-mercaptoethanol) was added to each lysate. The samples were then boiled for 5 min and electrophoresed on 12.5% SDS-polyacrylamide gels. Proteins were transferred to polyvinylidene fluoride membranes and, following blocking with 5% skim milk at room temperature for 30 min, immunoblotted with anti-c-Myc (9E10 hybridoma culture supernatant; Developmental Studies Hybridoma Bank, Iowa City, IA, USA) or anti-α-tubulin (cat. no. T5168; Merck KGaA, Darmstadt, Germany). Signals were detected with enhanced chemiluminescence using Western Lightning Plus-ECL reagent (PerkinElmer, Inc., Waltham, MA, USA) or Immobilon Western Chemiluminescent HRP substrate (Merck KGaA), and exposed to RX-U films (Fujifilm, Tokyo, Japan) in a dark room. The 9E10 hybridoma culture supernatant was diluted 1:50 in a washing buffer (19.8 mM Tris-HCl pH 7.6, 137 mM NaCl, and 0.1% Tween-20) containing 5% skim milk.

Detection of secreted Rspo2. Cells were washed with PBS twice, and then cultured in serum-free DMEM for 24 h with or without 50 μg/ml soluble heparin. The conditioned media was collected, and cell lysates were prepared as described above. The conditioned media was concentrated using Ni-nitrilotriacetic acid (Ni-NTA) agarose (Roche Diagnostics, Mannheim, Germany) for 2 h at 4˚C. Then, the Ni-NTA agarose was collected, washed with PBS twice, and eluted with buffer I (900 mM NaCl, 2.7 mM KCl, 10 mM Na_2HPO_4, 1.8 mM KH2PO4, and 500 mM imidazole). After being eluted from the Ni-NTA agarose, the amount of protein in each sample of conditioned media was estimated from the total amount of protein in each set of cell lysates by CBB staining. Based on the inverse ratio of each cell lysate concentration, additional buffer I was added to each sample to establish uniform concentrations among the conditioned media. Loading buffer was added to the conditioned media and cell lysates, and boiled for 5 min. Then, the proteins were separated by 12.5% SDS-PAGE and analyzed by immunoblotting with anti-c-Myc and anti-α-tubulin antibodies, as aforementioned.

Purification of recombinant Rspo2 for LC-MS. To purify recombinant Rspo2, a slightly modified version of a previously described method was used (35). Clonal HT1080 or A549 cells that expressed high levels of wild-type Rspo2-MH were established and cultured for 24 h in serum-free medium that contained 25 μl/ml heparin sepharose 6 fast flow (GE Healthcare Life Sciences, Little Chalfont, UK). Then, the heparin sepharose was collected, washed with PBS twice, and eluted with buffer II (900 mM NaCl, 2.7 mM KCl, 10 mM Na_2HPO_4, 1.8 mM KH_2PO_4, and 5 mM imidazole). The eluted samples were concentrated using Ni-NTA agarose for 2 h at 4˚C. The Ni-NTA agarose was collected, washed with buffer II, and eluted with buffer I by incubating for 5 min at room temperature followed by boiling for 5 min. The eluted samples were further concentrated on a Vivaspin 500 (3000 MWCO; Sartorius AG, Göttingen, Germany). The eluates were electrophoresed on an SDS-polyacrylamide gel, and the protein bands were visualized by CBB staining.

LC-MS. To identify the *C*-mannosylation sites, an ultrasensitive Q-Exactive nanoLC-MS/MS system was used. Purified Rspo2 samples were subjected to 12.5% SDS-PAGE. After CBB staining, the visible band was excised and de-stained. Following reduction and S-carboxymethylation with iodoacetic acid, in-gel digestion was performed using trypsin (TPCK-treated; Worthington Biochemical, Worthington, OH, USA) and an endoproteinase Asp-N (sequencing-grade; Roche Diagnostics, Basel, Switzerland). The digestion mixture was separated on a nanoflow LC (Easy nLC; Thermo Fisher Scientific, Inc.) using a nano-electrospray ionization spray column (NTCC analytical column; C18, ϕ75 μm x 100 mm, 3 μm; Nikkyo Technology Co., Ltd., Tokyo, Japan) with a linear gradient of 0-66% buffer B (100% acetonitrile and 0.1% formic acid) and a flow rate of 300 nl/min over 20 min, coupled on-line to a Q-Exactive mass spectrometer (Thermo Fisher Scientific, Inc.) that was equipped with a nanospray ion source that had no gas assistance. The mass spectrometer was operated in positive-ion mode, and the MS/MS spectra were acquired using an inclusion list that contained double or triple charged peptide ions with or without the *C*-mannosylation (^{146}EVGHWSEWGTCSR^{158} unmodified, m/z=796.3333 or 531.2247; mono-*C*-mannosylation, m/z=877.3598 or 585.2423; di-*C*-mannosylations, m/z=958.3862 or 639.2599). The MS/MS chromatograms of the y5 ion (m/z=581.2350±10 ppm) of the listed peptides and their MS/MS spectra were constructed using Qual Browser Thermo Xcalibur 3.1.66.10 (Thermo Fisher Scientific, Inc.).

Immunofluorescence. Cells were grown on coverslips in a 6-well plate, washed twice with PBS, fixed in 4% paraformaldehyde for 10 min, and permeabilized with 0.1% Triton X-100 for 10 min at room temperature. After being blocked with 3% bovine serum albumin for 30 min, the cells were incubated with anti-c-Myc at room temperature for 1 h. Alexa Fluor488-conjugated anti-mouse immunoglobulin (Ig)G (cat. no. A11029; Thermo Fisher Scientific, Inc.) was used as the secondary antibody at room temperature for 1 h. To determine the localization of the Golgi apparatus and the endoplasmic reticulum (ER), cells were incubated with a rabbit polyclonal anti-Golgi reassembly stacking protein 1 (GRASP65; cat. no. sc-30093; Santa Cruz Biotechnology, Inc., Dallas, TX., USA) and a rabbit polyclonal anti-calnexin (cat. no. 2433; Cell Signaling Technology, Inc., Danvers, MA, USA) antibody at room temperature for 1 h each. Alexa Fluor568-conjugated anti-rabbit IgG (cat. no. A11036; Thermo Fisher Scientific, Inc.) was used as the secondary antibody at room temperature for 1 h. After being washed twice with PBS, the cells were incubated with 2 μg/ml Hoechst 33258 (Polysciences, Inc., Warrington, PA, USA) for 10 min to stain the nuclei. Cells were then washed again three times with PBS and observed under a FLUOVIEW FV10i confocal laser-scanning microscope (Olympus Corporation, Tokyo, Japan). The 9E10 hybridoma culture supernatant towards c-Myc was diluted 1:4, while the anti-GRASP65 and anti-calnexin antibodies were diluted 1:100 in PBS containing 3% bovine serum albumin. The secondary antibodies were diluted 1:500 in PBS containing 3% bovine serum albumin.

Luciferase reporter assay. To assess Wnt/β-catenin signaling activity, a TOP/FOP luciferase reporter system was used. Each cell ($4x10^4$ cells/well) was seeded in 24-well plates and cultured overnight. Using the Lipofectamine 3000 transfection kit, the cells were transiently transfected with 800 ng canonical Wnt signaling reporter Super 8xTopFlash or mutant reporter Super 8xFopFlash (cat. nos. 12456 and 12457; Addgene, Watertown, MA, USA) (45) and 20 ng phRL-TK (Promega Corporation) in the presence of 30% Wnt3a-conditioned medium from L-Wnt3a cells (cat. no. CRL-2647; American Type Culture Collection, Manassas, VA, USA), as previously described (46). After 24 h, the cells were lysed, and firefly and Renilla luciferase activities were measured using infinite 200Pro multifunctional microplate reader (Tecan Group Ltd., Männedorf, Switzerland). TOPFlash and FOPFlash activities were normalized to that of *Renilla*.

Wound-healing assay. HT1080 and A549 cells ($2x10^5$ cells/well) were seeded into 24-well plates and cultured for 24 h to ~90% confluence, and then wounded using a yellow pipette tip. After being washed twice with PBS to remove floating cells, the cells were cultured in serum-free DMEM for 12 h (HT1080) or 96 h (A549). Photographs were captured of four independent areas, and the migrated areas were quantified using ImageJ 1.51 software (National Institutes of Health, Bethesda, MD, USA) (47).

Transwell migration assay. To assess migration, 6.5-mm transwell inserts with 8.0 μm pore polycarbonate membranes were used (cat. no. 3422; Corning, Inc., Corning, NY, USA). Cells were washed twice with serum-free DMEM to remove serum and seeded into the upper chambers at $2x10^4$ cells/chamber; the lower chambers were filled with growth medium. The cells were incubated for 3 h, and then non-migrated cells on the upper surfaces of the membranes were carefully removed with a cotton swab. Migrated cells were fixed and stained using Diff-Quick solution (Sysmex Corporation, Kobe, Japan). Photographs were capture from four independent areas and migration was quantified as the average number of migrated cells per area (48).

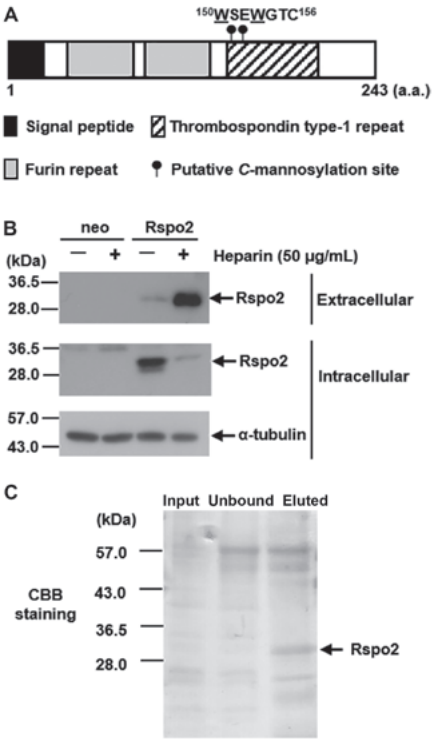

Figure 1. Purification of recombinant Rspo2 protein. (A) Schematic of human Rspo2. The locations of two putative *C*-mannosylation sites (Trp^{150} and Trp^{153}) are indicated by the black circles. (B) Establishment of Rspo2-overexpressing cell lines, HT1080-Rspo2-MH. HT1080-neo (neo) and HT1080-Rspo2-MH (Rspo2) were cultured in serum-free DMEM with or without 50 μg/ml soluble heparin for 24 h. The cell lysates and conditioned media were electrophoresed and immunoblotted with anti-c-Myc or anti-α-tubulin. (C) Purification of recombinant Rspo2. HT1080-Rspo2-MH cells were cultured in serum-free DMEM with 25 μl/ml heparin sepharose 6 Fast Flow for 24 h, and heparin sepharose was collected. Heparin sepharose-bound proteins were eluted, and eluates were further purified with Ni-NTA agarose. The samples obtained were electrophoresed on an SDS-polyacrylamide gel. The gels were visualized by CBB staining. Rspo2, R-spondin2; Trp, tryptophan; Ni-NTA, Ni-nitrilotriacetic acid; CBB, coomassie brilliant blue.

Statistical analysis. Data were expressed as the mean ± standard deviation of three independent experiments. Statistical analyses were performed using one-way analysis of variance with Tukey's post-hoc test. Analysis was performed with GraphPad Prism 8 statistical software (GraphPad Software, Inc., La Jolla, CA, USA). $P<0.05$ was considered to indicate a statistically significant difference.

Results

Rspo2 is C-mannosylated at Trp^{150} and Trp^{153}. Human Rspo2 has two consecutive *C*-mannosylation consensus sequence sites from Trp^{150} (W^{150}-S-E-W^{153}-G-T-C) in the TSR1 domain (Fig. 1A). To determine whether these tryptophans are

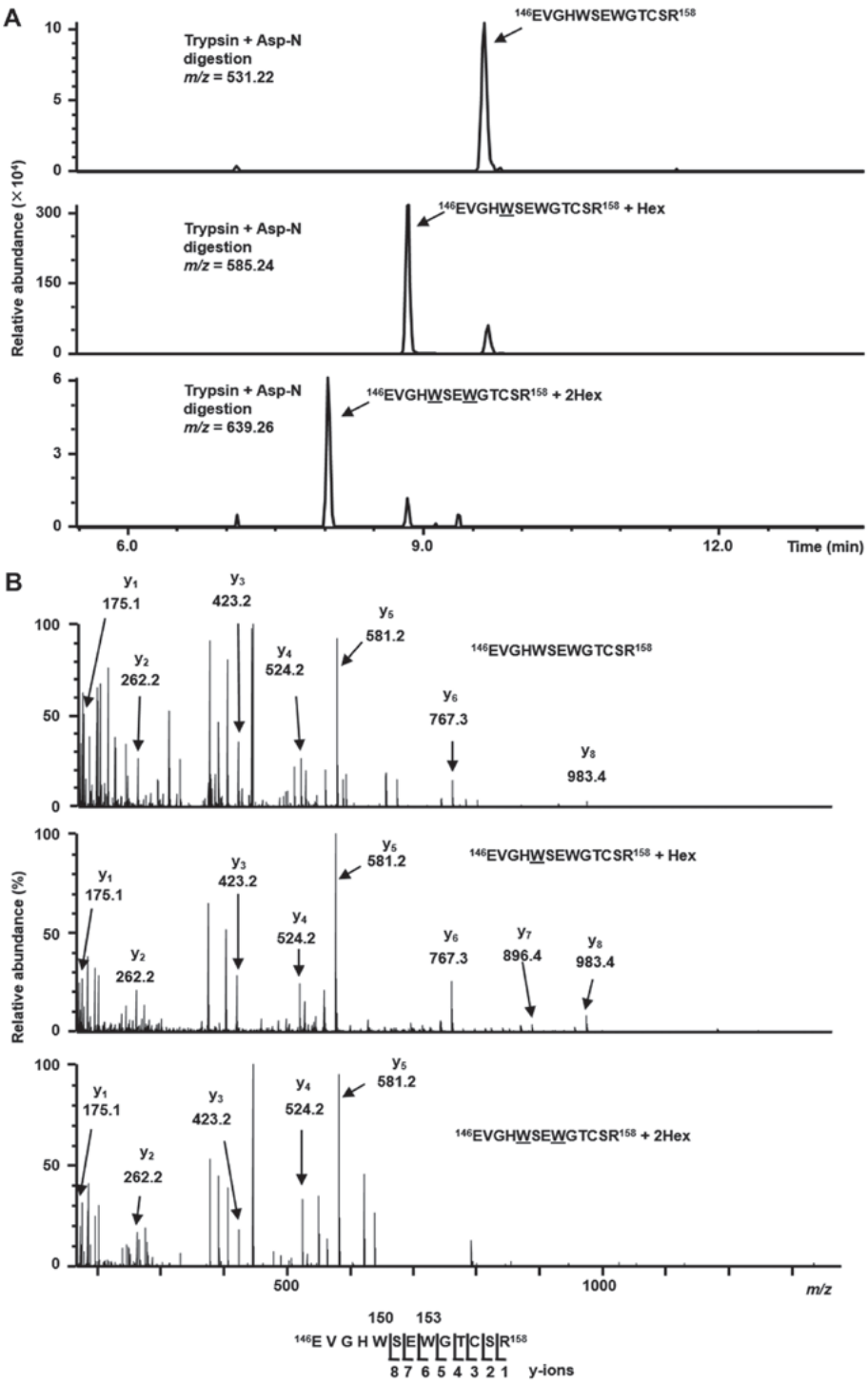

Figure 2. Trp[150] and Trp[153] of Rspo2 are *C*-mannosylated. (A) Purified recombinant Rspo2 protein samples were digested with trypsin and Asp-N, and the resulting peptides were analyzed by targeted MS/MS. According to the inclusion list of triple protonated ions of un-, mono-, and di-mannosylated [146]EVGHWSEWGTCSR[158] peptides (*m/z*=531.22, 585.24 and 639.26, respectively), MS/MS spectra were obtained, and selected ion chromatograms of y5 ions (*m/z*=581.24) of these parent ions were drawn. (B) MS/MS spectra of the triple-charged un-, mono-, and di-mannosylated [146]EVGHWSEWGTCSR[158] peptides (*m/z*=531.22, 585.24 and 639.26, respectively). The indicated y-ions were detected as single charged ions. Un-mannosylated- (top), only Trp[150]-mannosylated- (middle), and both Trp[150]- and Trp[153]-mannosylated- (bottom) peptides were observed. Trp, tryptophan; Rspo2, R-spondin2; MS/MS, tandem mass spectroscopy.

C-mannosylated, a Rspo2-overexpressing HT1080 clonal cell line was established (HT1080-Rspo2-MH). Because the R-spondin family proteins bind to cell surface heparan sulfate proteoglycans (14,49), to confirm that Rspo2 is secreted in the conditioned medium, cells were treated with heparin. As a result, the levels of secreted Rspo2 were increased (Fig. 1B). Therefore, sequential affinity chromatography was performed using heparin sepharose and Ni-NTA agarose to purify the recombinant Rspo2 (Fig. 1C).

The resulting purified sample was digested with trypsin and Asp-N, and the subsequent mixture of peptides was subjected to LC-MS. LC-MS analysis indicated a triply charged form of the peptide [146]EVGHWSEWGTCSR[158], corresponding to un-, mono-, and di-mannosylated forms (Fig. 2A). The expected

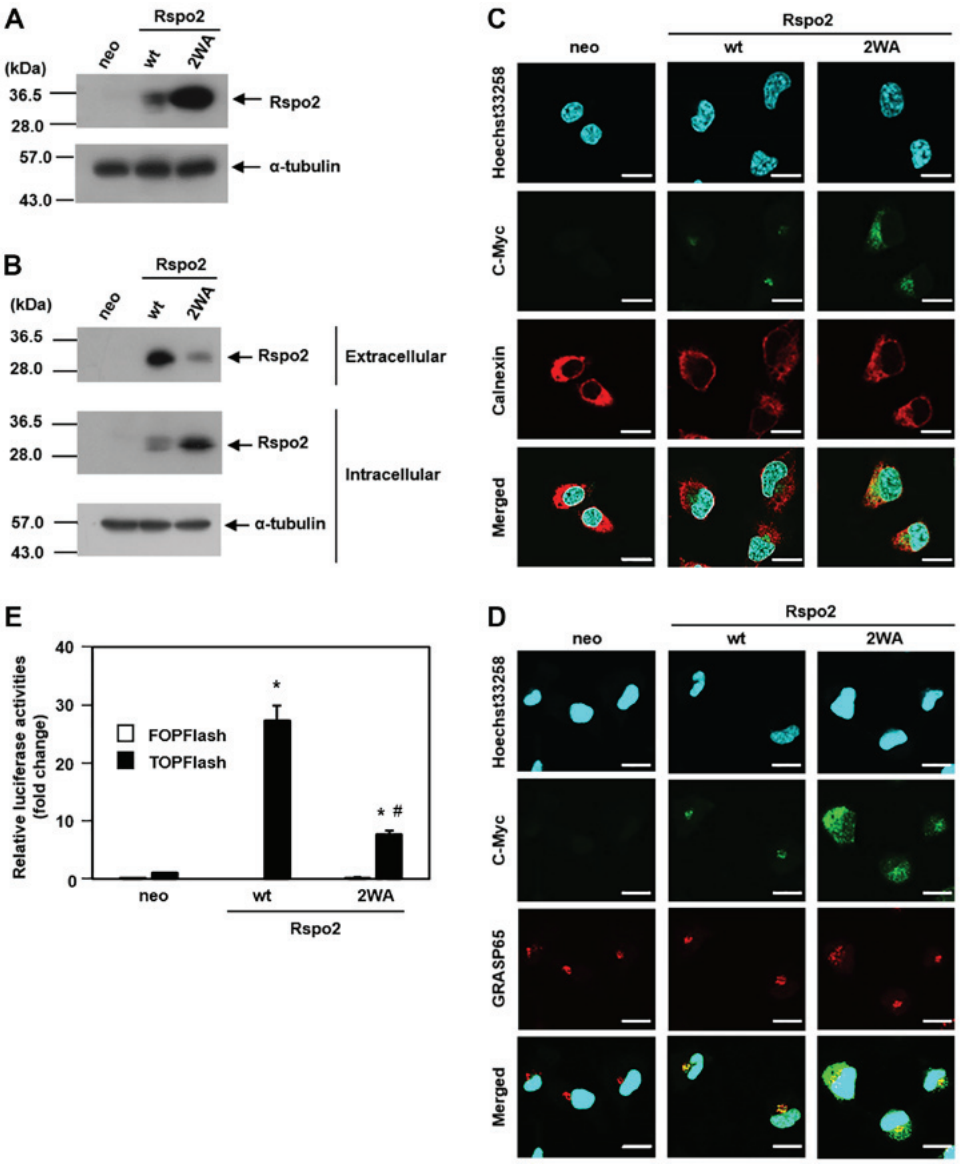

Figure 3. Rspo2 functions are regulated by *C*-mannosylation. (A) A *C*-mannosylation-defective mutant form of Rspo2 was generated (2WA) and overexpressed in the HT1080 cell line (HT1080-Rspo2/2WA-MH). Control HT1080-neo (neo), HT1080-Rspo2-MH (wt), and HT1080-Rspo2/2WA-MH (2WA) cells were lysed, and each cell lysate was electrophoresed and immunoblotted with anti-c-Myc and anti-α-tubulin. (B) Effect of *C*-mannosylation on Rspo2 secretion. Each cell line was cultured in serum-free medium with 50 μg/ml heparin. After 24 h, each batch of cell lysates and conditioned media were collected, and the samples were electrophoresed and immunoblotted with anti-c-Myc or anti-α-tubulin. (C) Effect of *C*-mannosylation on the intracellular trafficking of Rspo2. Each cell line was fixed and stained with Hoechst33258 (blue), anti-c-Myc (green), and anti-calnexin (red). The samples were observed under a confocal laser-scanning microscope and representative photographs were captured under identical magnification (magnification, x60), microscope conditions and linear adjustment. Scale bar, 20 μm. (D) Effect of C-mannosylation on the intracellular trafficking of Rspo2. Each cell line was fixed and stained with Hoechst33258 (blue), anti-c-Myc (green), and anti-GRASP65 (red). The samples were observed under a confocal laser-scanning microscope and representative photographs were captured under identical magnification (magnification, x60), microscope conditions and linear adjustment. Scale bar, 20 μm. (E) Effect of *C*-mannosylation on Rspo2-mediated enhancement of Wnt signaling. Each cell line was transfected with TOPFlash or FOPFlash in the presence of 30% L-Wnt3a cell-conditioned medium. After 24 h, luciferase activities were measured and normalized to *Renilla* luciferase. *P<0.05 compared with neo; $^{\#}$P<0.05 compared with wt. Rspo2, R-spondin2; wt, wild-type; GRASP65, Golgi reassembly stacking protein 1.

values of *m/z* for each peptide are 531.22, 585.24 and 639.26, respectively, and each peptide was detected at the expected *m/z*, suggesting that Rspo2 exists in un-, mono-, and di-mannosylated forms. In addition, to identify the *C*-mannosylation sites of Rspo2, LC-MS/MS analysis was performed on the aforementioned peptides (Fig. 2B). The un- and mono-mannosylated peptides had the same spectral pattern until the y8 ions. This result suggested that one mannose was modified in ^{146}EVGHW^{150}. Based on previous studies, there is no indication that any hexose modification occurs in those peptides, except at Trp^{150}. Thus, it is most likely that Trp^{150} is mannosylated. Then, the di-mannosylated peptide was identified from the y1 ion to the y5 ion by LC-MS/MS analysis, indicating that two mannoses are modified in ^{146}EVGHWSEW^{153}. Considering that un- and mono-mannosylated peptides were identified from the y1 ion to the y8 ion, it was concluded that Trp^{153} was modified. In addition, Trp^{150} was likely modified by one mannose residue; one- and two-hexose glycosylation at Glu, Val, Gly, His, and Ser have not been reported. Furthermore, to verify whether Rspo2 is also *C*-mannosylated in other cell types, a

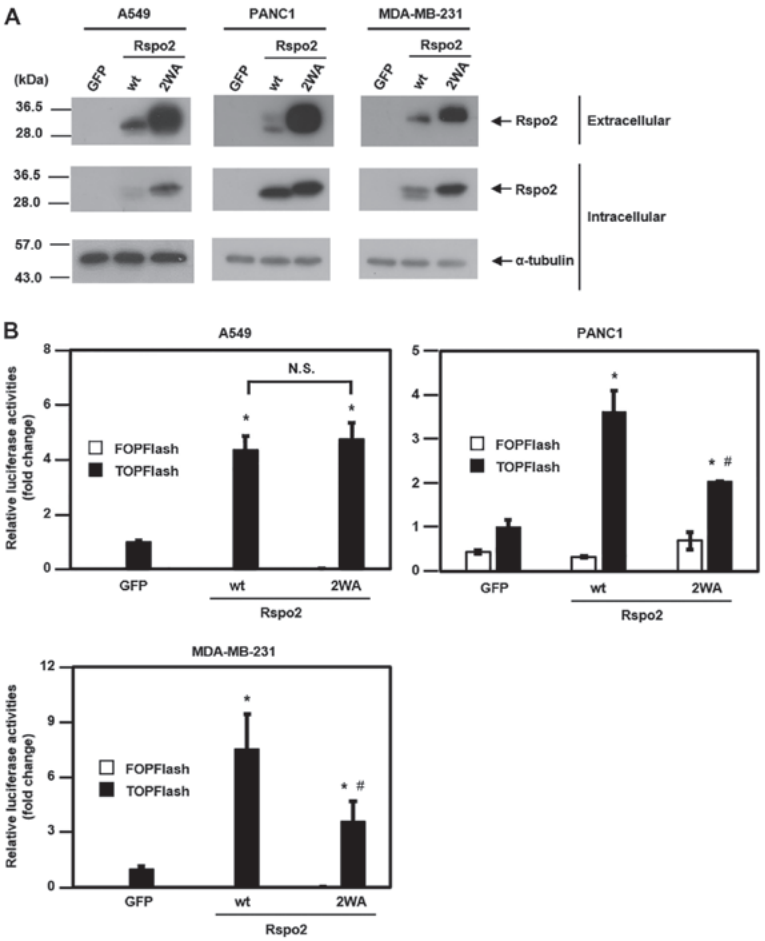

Figure 4. Rspo2 functions are regulated by *C*-mannosylation in certain tumor cell lines. (A) Effects of *C*-mannosylation on Rspo2 secretion in A549, PANC1 and MDA-MB-231 cells. Each Rspo2-overexpressing cell line was cultured in serum-free DMEM with 50 μg/ml heparin. After 24 h, each batch of cell lysates and conditioned media were collected, and the samples were electrophoresed and immunoblotted with anti-c-Myc or anti-α-tubulin. (B) Effect of *C*-mannosylation on Rspo2-mediated enhancement of Wnt signaling in A549, PANC1 and MDA-MB-231 cells. Each cell line was transfected with TOPFlash or FOPFlash in the presence of 30% L-Wnt3a cell-conditioned medium. After 24 h, luciferase activities were measured and normalized to Renilla luciferase. *P<0.05 compared with control cells (GFP); $^{\#}$P<0.05 compared with wt. Rspo2, R-spondin2; wt, wild-type; GFP, green fluorescent protein; ns, not significant.

Rspo2-overexpressing clonal cell line was generated in A549 cells (A549-Rspo2-MH) and recombinant Rspo2 was purified. As presented in Fig. S1, Rspo2 was also *C*-mannosylated in A549 cells. Altogether, Rspo2 was demonstrated to exist in three forms: un-mannosylated, Trp^{150}-mannosylated, and Trp^{150}- and Trp^{153}-mannosylated. Therefore, it was concluded that both Trp^{150} and Trp^{153} were *C*-mannosylation sites of Rspo2 in human tumor cells.

C-mannosylation of Rspo2 regulates its secretion and intracellular trafficking in HT1080 cells. Glycoproteins often regulate their secretion by glycosylation. Because Rspo2 is secreted into the extracellular environment, we examined whether *C*-mannosylation of Rspo2 regulates its secretion. To this end, a *C*-mannosylation-defective mutant Rspo2-overexpressing HT1080 clonal cell line was generated (HT1080-Rspo2/2WA-MH) by substituting the two Trps, Trp^{150} and Trp^{153}, with Ala. This cell line was confirmed by western blot analysis (Fig. 3A).

Firstly, western blotting was performed to compare secretory levels between wild-type and 2WA Rspo2. The results indicated that the secretory levels of the *C*-mannosylation-defective 2WA mutant Rspo2 decreased compared with wild-type Rspo2 (Fig. 3B). Because secretory proteins must be able to move from the ER to the Golgi apparatus (50), it was hypothesized that the defect in *C*-mannosylation of Rspo2 may have affected its intracellular localization, resulting in less secretion and increased accumulation of Rspo2/2WA in the cell lysate. Using antibodies against calnexin, an ER marker, and GRASP65, a marker for the Golgi apparatus, immunofluorescence staining was performed in order to examine the localization of wild-type and 2WA localization in the ER or Golgi apparatus. As expected, whereas wild-type Rspo2 localized to the Golgi apparatus, Rspo2/2WA accumulated in the ER (Fig. 3C and D). These data indicated that *C*-mannosylation of Rspo2 was important for its transportation from the ER to the Golgi apparatus.

C-mannosylation of Rspo2 mediates agonistic activity in Wnt/β-catenin signaling in HT1080 cells. R-spondin proteins, including Rspo2, have been reported to be agonists of Wnt/β-catenin signaling (2,4-8). Because *N*-glycosylation of Wnt3a is necessary for its function and subsequent signaling (51), it was examined whether *C*-mannosylation of Rspo2 affects its agonistic activity in the Wnt/β-catenin signaling pathway. To measure Wnt/β-catenin signaling

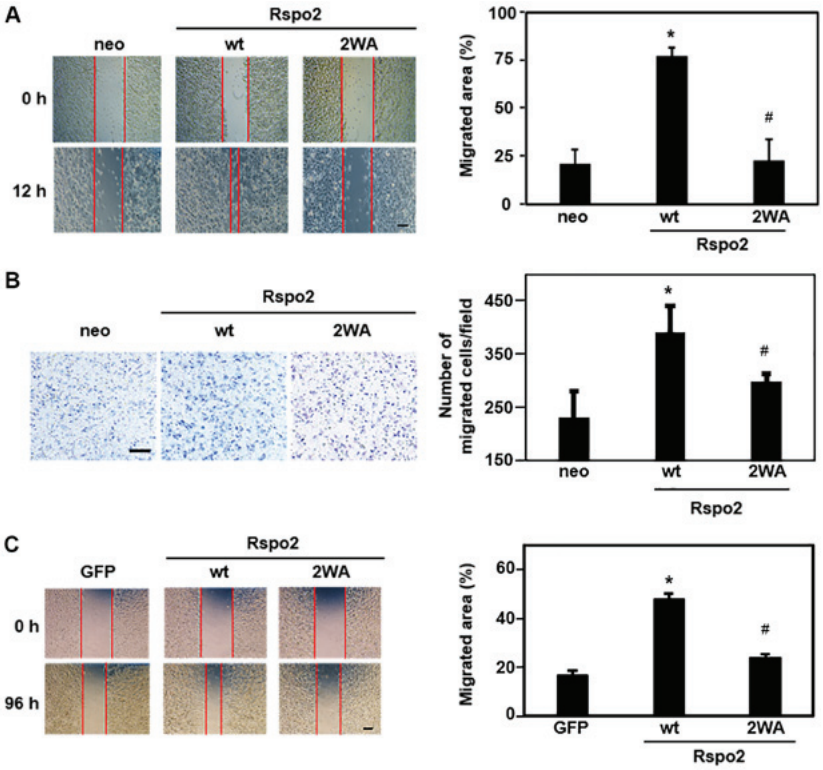

Figure 5. Effect of *C*-mannosylation on Rspo2-mediated cancer cell migration. (A) Wound-healing assay of Rspo2-overexpressing HT1080 cells. Cells were scratched and photographed under an inverted microscope at 0 and 12 h post-wounding. Photographs were captured at four independent areas. Representative images and quantitative analysis of the relative area of migration are shown. Scale bar, 100 μm. (B) Transwell migration assay of Rspo2-overexpressing HT1080 cells. Cells were seeded into transwell chambers and cultured for 3 h. After 3 h, non-migrated cells were removed with a cotton swab, and migrated cells were visualized by Diff-Quick staining. Stained cells were observed by inverted microscopy, and photographs were captured at four independent areas (magnification, x10). Representative images and quantitative analysis are shown. Scale bar, 100 μm. (C) Wound-healing assay of Rspo2-overexpressing A549 cells. Cells were scratched and photographed by inverted microscopy at 0 and 96 h post-wounding. Photographs were captured at four independent areas. Representative images and quantitative analysis of the relative area of migration are shown. Scale bar, 100 μm. *P<0.05 compared with control (neo or GFP); $^{\#}$P<0.05 compared with wt. Rspo2, R-spondin2; wt, wild-type; GFP, green fluorescent protein.

activity, a luciferase reporter assay was used. TOPFlash, which has seven tandem repeats of the TCF/LEF binding motifs upstream of the firefly luciferase gene, was transfected into each Rspo2-overexpressing HT1080 clonal cell line, and luciferase activity was measured. Transfected cells were cultured in Wnt3a-containing medium for 24 h. Although both wild-type and 2WA Rspo2-overexpressing cell lines displayed increased TOPFlash activity compared with control cells, the activity in wild-type cells was increased by 27.3-fold compared with only 7.8-fold in 2WA cells (Fig. 3E). Thus, the *C*-mannosylation-defective Rspo2/2WA had reduced TOPFlash activity compared with the wild-type Rspo2.

Effect of C-mannosylation on Rspo2 functions in other human tumor cell lines. To confirm the role of *C*-mannosylation on Rspo2 functions in cancer, three additional human tumor cell lines were used, namely A549, PANC1 and MDA-MB-231. First, wild-type and 2WA mutant Rspo2-overexpressing A549, PANC1 and MDA-MB-231 cell lines were established, and then the secretory levels of these proteins were assessed. Notably, the secretory levels of the *C*-mannosylation-defective 2WA mutant Rspo2 were increased compared with wild-type Rspo2 in A549, PANC1 and MDA-MB-231 cells (Fig. 4A). Next, the effect of *C*-mannosylation on Rspo2-mediated activation of Wnt/β-catenin signaling was examined in these cell lines. The results demonstrated that the TOPFlash activity of 2WA mutant Rspo2-overexpressing cells was reduced compared with wild-type Rspo2-overexpressing cells in PANC1 and MDA-MB-231 cell lines (Fig. 4B), similar to the aforementioned results in HT1080 cells. No difference in TOPFlash activity was observed, however, in Rspo2/wild-type- and Rspo2/2WA-overexpressing A549 cells (Fig. 4B). Therefore, the present results suggested that *C*-mannosylation may be important for the Wnt/β-catenin signaling-enhancing activity of Rspo2 in HT1080, PANC1 and MDA-MB-231 cells.

C-mannosylation of Rspo2 regulates cancer cell migration. Because, Rspo2 contributes to cancer progression (18-20), it was next examined whether *C*-mannosylation of Rspo2 may regulate cancer cell migration *in vitro*. Confluent Rspo2-overexpressing HT1080 clonal cells were subjected to wound-healing assays, and 12 h post-scratching, wound closure areas were quantified. As presented in Fig. 5A, the overexpression of wild-type Rspo2 significantly increased cell migration compared with control cells, whereas overexpression of 2WA mutant Rspo2 had little effect on migration. Similar results were obtained with transwell migration assays (Fig. 5B).

To confirm that *C*-mannosylation of Rspo2 may mediate migration of other cancer cell lines, Rspo2-overexpressing A549 clonal cells were used. Using a wound-healing assay,

cell migration ability was demonstrated to be increased in A549-Rspo2/wild-type, compared with control cells, but was unchanged in A549-Rspo2/2WA cells (Fig. 5C). These results indicate that *C*-mannosylation of Rspo2 regulated the migration of HT1080 and A549 cells. In addition, the present findings demonstrated that a defect in the *C*-mannosylation of Rspo2 abrogated its ability to mediate cancer cell migration.

C-mannosylation of Rspo2 at Trp^{150} is important for Wnt/β-catenin signaling activation. Although the present results demonstrated that Rspo2 is *C*-mannosylated at Trp^{150} and Trp^{153}, Rspo2 was observed in un-mannosylated (4%), Trp^{150}-mannosylated (94%), and Trp^{150}- and Trp^{153}-mannosylated (2%) forms (Fig. 2A). Therefore, it can by hypothesized that single *C*-mannosylation at Trp^{150} may be more important for Rspo2 functions, compared with the di-mannosylated form. Therefore, Trp^{150}-*C*-mannosylation-defective mutant Rspo2-overexpressing HT1080 cells were generated (HT1080 Rspo2/W150A-MH) and compared with the other Rspo2-overexpressing HT1080 cells for their ability to activate Wnt/β-catenin signaling. The results demonstrated that Rspo2/W150A had reduced TOPFlash activity compared with the wild-type Rspo2, but exhibited comparable activity with the Rspo2/2WA mutant (Fig. S2). These results suggested that *C*-mannosylation at Trp^{150} may be more important than Trp^{153} for Rspo2 functions.

Discussion

C-mannosylation is a unique type of glycosylation that contributes to proper secretion, protein folding, and protein-protein interactions (29-32). Recently, Hendee *et al* (52) reported that the *C*-mannosylated Trp^{42} of ADAMTS like 1 protein is often mutated to Arg in a human pedigree that is affected by eye diseases, such as developmental glaucoma. Their study is the first to suggest an association between abnormal *C*-mannosylation and disease; however, because there are fewer reports on *C*-mannosylation and *C*-mannosylated proteins than other types of glycosylation, the function of *C*-mannosylation, particularly in cancer progression, is unknown.

The present study focused on Rspo2, which has two putative *C*-mannosylation sites in the TSR1 domain, and determined that Trp^{150} and Trp^{153} were *C*-mannosylated by LC-MS/MS. *C*-mannosylation affected the extracellular secretion of Rspo2 and its intracellular trafficking from the ER to the Golgi apparatus (Figs. 3B-D and 4A). Furthermore, it regulated the agonistic activity of Wnt/β-catenin signaling and cancer cell migration (Figs. 3E, 4B and 5). Although an increase in mass due to the attachment of mannose and the characteristic cross-ring cleavage (53) was not detected in HT1080 cells (Fig. 2B), MS/MS spectra of Rspo2 purified from Rspo2-overexpressing A549 cells exhibited hexose attachment and characteristic cross-ring cleavage (Fig. S1). In the mono-mannosylated peptide, addition of 162 kDa (one mannose residue) was detected in the y9 ion, but not in the y7 and y8 ions (Fig. S1), clearly indicating that this modification occurred at Trp^{150}. Furthermore, in the di-mannosylated peptide, one hexose attachment and a characteristic cross-ring cleavage were detected in the y8 ion (Fig. S1), but not in the y1-y5 ions (data not shown). These results indicated that one *C*-mannosylated amino acid residue existed among Ser^{151}, Glu^{152} and Trp^{153}. Based on previous studies, it is most likely that Trp^{153} was *C*-mannosylated. Furthermore, since Trp^{150} was *C*-mannosylated at the mono-mannosylated peptide, the other hexose attachment in the di-mannosylated peptide had most likely occurred at Trp^{150}. The possibility of other glycosylations may be excluded for the following three reasons: *N*-mannosylation is observed only in insects and fungus (54,55); *O*-mannosylation at Ser/Thr residues is further elongated by some saccharides; and *O*-glucosylation and *O*-galactosylation have not been reported in the residues of ^{146}EVGHW^{150}, and these glycosylations occur primarily in Notch protein and collagen, respectively (56). Thus, it was concluded from the present results that the Trp^{150} and Trp^{153} residues of Rspo2 were *C*-mannosylated.

Next, the present study examined whether *C*-mannosylation affected the functions of Rspo2 by establishing wild-type Rspo2-overexpressing cells and *C*-mannosylation-defective mutant Rspo2/2WA-overexpressing cells. Because Rspo2 is a secreted protein and a ligand that activates Wnt/β-catenin signaling (2,5-8), it was determined whether *C*-mannosylation alters its secretion. The results demonstrated that secretion of Rspo2/2WA was reduced in HT1080 cells, but increased in A549, PANC1 and MDA-MB-231 cells (Figs. 3B and 4A). These findings prompted us to examine its intracellular localization. Because *C*-mannosylation occurs in the ER lumen (57,58), it was hypothesized that changes in glycosylation may affect the intracellular trafficking of Rspo2. As expected, a deficiency in *C*-mannosylation of Rspo2 resulted in its accumulation in the ER in HT1080 cells (Fig. 3C and D), suggesting that *C*-mannosylation was required for intracellular trafficking from the ER to the Golgi apparatus. In addition, the intracellular mutant Rspo2 expression levels were significantly increased compared with the wild-type. As Rspo2 bound to the cell surface (secreted Rspo2) is dissociated by heparin, it is presumed that these greater levels were also caused by its accumulation in the ER. However, the effect of *C*-mannosylation on the intracellular trafficking of Rspo2 in the other cell lines examined, namely A549, PANC1 and MDA-MB-231 cells, was similar to the HT1080 cells (data not shown), which was inconsistent with the secretory effects. Since Rspo2 has an opposite function on cancer progression depending on the type of cancer (18-20), it is possible that Rspo2 secretion may be different in the different tumor cell lines, and that the effect of *C*-mannosylation may be dependent on the type of tumor cell line. Further studies on the effects of *C*-mannosylation on the secretion of Rspo2 in additional cell lines, and a deeper understanding of the mechanisms involved, will be required in the future.

Wnt/β-catenin signaling is activated by the interaction between Rspo2, LGR4-6 and ZNRF3/RNF43 (2,5-8). Because it was observed that a defect in the *C*-mannosylation of Rspo2 decreased its agonistic activity in the Wnt/β-catenin signaling pathway (Fig. 3E and 4B), it is likely that the binding of Rspo2 to its receptors was also reduced. It is possible that the significant decrease in Wnt/β-catenin signaling in Rspo2/2WA may be due to the lower secretion in HT1080 cells (Fig. 3B). However, whereas the secretory levels of Rspo2/2WA were increased in PNAC1 and MDA-MB-231 cells (Fig. 4A),

their TOPFlash activities were reduced compared with Rspo2/wild-type cells (Fig. 4B). These results suggested that *C*-mannosylated Rspo2 had stronger activity compared with the *C*-mannosylation-defective Rspo2. Furthermore, *C*-mannosylation of Rspo1 has been reported to enhance Wnt/β-catenin signaling, regardless of its secretory level (30). Further experiments will be required in the future to confirm the effects of *C*-mannosylation in the secreted form of Rspo2, by using purified wild-type and mutant Rspo2. The present results, nonetheless, indicated that *C*-mannosylation of Rspo2 may have contributed to its agonistic activity in the Wnt/β-catenin signaling pathway, more than to its regulation of secretion.

Rspo2 is involved in cancer progression as an enhancer and a suppressor (18-20). The present results demonstrated that Rspo2 enhanced cell migration in two distinct cancer cell lines: Human lung adenocarcinoma A549 and human fibrosarcoma HT1080 (Fig. 5). By contrast, Dong *et al* (36) reported that Rspo2 has a suppressive effect on cancer progression in human colorectal cancer LoVo cells. Thus, to confirm these results, a Rspo2-overexpressing LoVo cell lines was generated and the results demonstrated that overexpression of Rspo2 suppressed the migration of LoVo cells (data not shown), similar to the previous report (36). These findings suggested that Rspo2 may have opposing functions on cancer progression. Subsequently, it was examined whether *C*-mannosylation was associated with migration. Migration was impeded in Rspo2/2WA-overexpressing cells (Fig. 5), suggesting that the *C*-mannosylation of Rspo2 enhanced cell migration in certain tumor cell lines. To further elucidate the role of *C*-mannosylation on Rspo2 and cancer progression, *in vivo* studies will be required in the future.

Finally, as the majority (94%) of all secreted Rspo2 was demonstrated to have a *C*-mannosylation at Trp^{150}, it was hypothesized that this modification had an important effect on Rspo2 functions. Regarding a Trp^{153}-*C*-mannosylation-defective mutant Rspo2, substitution of Trp^{153} to Ala would result in the disruption of the consensus sequence of Trp^{150}-*C*-mannosylation. In addition, because Cys^{156} is predicted to form a disulfide bond, replacing this Cys to break the consensus sequence against Trp^{153} may induce other effects independent of the *C*-mannosylation at Trp^{153}. Therefore, only a Rspo2/W150A mutant was constructed and overexpressed in HT1080 cells and its effects on Wnt/β-catenin agonistic activity were compared with the Rspo2/wild-type- and Rspo2/2WA-overexpressing HT1080 cells. As expected, Rspo2/W150A and Rspo2/2WA-expressing cells had significantly reduced agonistic activity. This corresponded with the results regarding the role of Rspo3 *C*-mannosylation previously reported (35). Because Rspo1-4 have a conserved W-X-X-W-X-X-C sequence, these results suggested that *C*-mannosylation at the first Trp residue of the above sequence may have a common important role in R-spondin family proteins.

In conclusion, the present study demonstrated that Rspo2 is *C*-mannosylated at Trp^{150} and Trp^{153} and that this modification regulated certain functions of Rspo2. Wnt/β-catenin signaling is often abnormally activated in cancer progression, and cell migration is one of the features of tumor malignancy that is associated with cancer metastasis. Thus, the present findings indicated that the *C*-mannosylation of Rspo2 may serve as a novel therapeutic target and diagnostic marker in cancer.

Acknowledgements

We thank Dr Randall T Moon (University of Washington School of Medicine, Seattle, WA, USA) for providing Super 8x TopFlash and Super 8x FopFlash (45).

Funding

This study was supported by a Grant-in-Aid for Young Scientists (grant no. JP17K15094), a Grant-in-Aid for Scientific Research (grant no. JP18K06137), and the Amano Institute of Technology.

Availability of data and materials

The datasets used and/or analyzed during the present study are available from the corresponding author on reasonable request.

Authors' contributions

HM, KK, YN and SS designed the study. HM and KK performed the cell-based functional analysis. TS and ND performed the LC-MS analysis. HM, YN and SS wrote the manuscript. All authors read and approved the final manuscript.

Ethics approval and consent to participate

Not applicable.

Patient consent for publication

Not applicable.

Competing interests

The authors declare that they have no competing interests.

References

1. Kamata T, Katsube K, Michikawa M, Yamada M, Takada S and Mizusawa H: R-spondin, a novel gene with thrombospondin type 1 domain, was expressed in the dorsal neural tube and affected in Wnts mutants. Biochim Biophys Acta 1676: 51-62, 2004.
2. Kazanskaya O, Glinka A, del Barco Barrantes I, Stannek P, Niehrs C and Wu W: R-Spondin2 is a secreted activator of Wnt/β-catenin signaling and is required for *Xenopus* myogenesis. Dev Cell 7: 525-534, 2004.
3. de Lau WB, Snel B and Clevers HC: The R-spondin protein family. Genome Biol 13: 242, 2012.
4. Kim KA, Zhao J, Andarmani S, Kakitani M, Oshima T, Binnerts ME, Abo A, Tomizuka K and Funk WD: R-Spondin proteins: A novel link to β-catenin activation. Cell Cycle 5: 23-26, 2006.
5. Carmon KS, Gong X, Lin Q, Thomas A and Liu Q: R-spondins function as ligands of the orphan receptors LGR4 and LGR5 to regulate Wnt/β-catenin signaling. Proc Natl Acad Sci USA 108: 11452-11457, 2011.
6. de Lau W, Barker N, Low TY, Koo BK, Li VSW, Teunissen H, Kujala P, Haegebarth A, Peters PJ, van de Wetering M, *et al*: Lgr5 homologues associate with Wnt receptors and mediate R-spondin signalling. Nature 476: 293-297, 2011.

7. Glinka A, Dolde C, Kirsch N, Huang YL, Kazanskaya O, Ingelfinger D, Boutros M, Cruciat CM and Niehrs C: LGR4 and LGR5 are R-spondin receptors mediating Wnt/β-catenin and Wnt/PCP signalling. EMBO Rep 12: 1055-1061, 2011.
8. Hao HX, Xie Y, Zhang Y, Charlat O, Oster E, Avello M, Lei H, Mickanin C, Liu D, Ruffner H, *et al*: ZNRF3 promotes Wnt receptor turnover in an R-spondin-sensitive manner. Nature 485: 195-200, 2012.
9. Anastas JN and Moon RT: WNT signalling pathways as therapeutic targets in cancer. Nat Rev Cancer 13: 11-26, 2013.
10. Cisternas P, Henriquez JP, Brandan E and Inestrosa NC: Wnt signaling in skeletal muscle dynamics: Myogenesis, neuromuscular synapse and fibrosis. Mol Neurobiol 49: 574-589, 2014.
11. van Amerongen R and Berns A: Knockout mouse models to study Wnt signal transduction. Trends Genet 22: 678-689, 2006.
12. Kawakami Y, Rodriguez Esteban C, Raya M, Kawakami H, Martí M, Dubova I and Izpisúa Belmonte JC: Wnt/β-catenin signaling regulates vertebrate limb regeneration. Genes Dev 20: 3232-3237, 2006.
13. Nusse R and Clevers H: Wnt/β-Catenin signaling, disease, and emerging therapeutic modalities. Cell 169: 985-999, 2017.
14. Bell SM, Schreiner CM, Wert SE, Mucenski ML, Scott WJ and Whitsett JA: R-spondin 2 is required for normal laryngeal-tracheal, lung and limb morphogenesis. Development 135: 1049-1058, 2008.
15. Aoki M, Kiyonari H, Nakamura H and Okamoto H: R-spondin2 expression in the apical ectodermal ridge is essential for outgrowth and patterning in mouse limb development. Dev Growth Differ 50: 85-95, 2008.
16. Abed É, Chan TF, Delalandre A, Martel-Pelletier J, Pelletier JP and Lajeunesse D: R-spondins are newly recognized players in osteoarthritis that regulate Wnt signaling in osteoblasts. Arthritis Rheum 63: 3865-3875, 2011.
17. Han XH, Jin YR, Seto M and Yoon JK: A WNT/β-catenin signaling activator, R-spondin, plays positive regulatory roles during skeletal myogenesis. J Biol Chem 286: 10649-10659, 2011.
18. Wu C, Qiu S, Lu L, Zou J, Li WF, Wang O, Zhao H, Wang H, Tang J, Chen L, *et al*: RSPO2-LGR5 signaling has tumour-suppressive activity in colorectal cancer. Nat Commun 5: 3149, 2014.
19. Yin X, Yi H, Wang L, Wu W, Wu X and Yu L: R-spondin 2 promotes proliferation and migration via the Wnt/β-catenin pathway in human hepatocellular carcinoma. Oncol Lett 14: 1757-1765, 2017.
20. Ilmer M, Boiles AR, Regel I, Yokoi K, Michalski CW, Wistuba II, Rodriguez J, Alt E and Vykoukal J: RSPO2 enhances canonical Wnt signaling to confer stemness-associated traits to susceptible pancreatic cancer cells. Cancer Res 75: 1883-1896, 2015.
21. Krieg J, Hartmann S, Vicentini A, Gläsner W, Hess D and Hofsteenge J: Recognition signal for C-mannosylation of Trp-7 in RNase 2 consists of sequence Trp-x-x-Trp. Mol Biol Cell 9: 301-309, 1998.
22. Julenius K: NetCGlyc 1.0: Prediction of mammalian C-mannosylation sites. Glycobiology 17: 868-876, 2007.
23. Hofsteenge J, Müller DR, de Beer T, Löffler A, Richter WJ and Vliegenthart JFG: New type of linkage between a carbohydrate and a protein: *C*-glycosylation of a specific tryptophan residue in human RNase Us. Biochemistry 33: 13524-13530, 1994.
24. Niwa Y and Simizu S: *C*-mannosylation: Previous studies and future research perspectives. Trends Glycosci Glycotechnol 30: E231-E238, 2018.
25. Krieg J, Gläsner W, Vicentini A, Doucey MA, Löffler A, Hess D and Hofsteenge J: C-Mannosylation of human RNase 2 is an intracellular process performed by a variety of cultured cells. J Biol Chem 272: 26687-26692, 1997.
26. Morishita S, Suzuki T, Niwa Y, Dohmae N and Simizu S: Dpy-19 like 3-mediated *C*-mannosylation and expression levels of RPE-spondin in human tumor cell lines. Oncol Lett 14: 2537-2544, 2017.
27. Otani K, Niwa Y, Suzuki T, Sato N, Sasazawa Y, Dohmae N and Simizu S: Regulation of granulocyte colony-stimulating factor receptor-mediated granulocytic differentiation by *C*-mannosylation. Biochem Biophys Res Commun 498: 466-472, 2018.
28. Sasazawa Y, Sato N, Suzuki T, Dohmae N and Simizu S: *C*-Mannosylation of thrombopoietin receptor (c-Mpl) regulates thrombopoietin-dependent JAK-STAT signaling. Biochem Biophys Res Commun 468: 262-268, 2015.
29. Goto Y, Niwa Y, Suzuki T, Dohmae N, Umezawa K and Simizu S: *C*-mannosylation of human hyaluronidase 1: Possible roles for secretion and enzymatic activity. Int J Oncol 45: 344-350, 2014.
30. Niwa Y, Suzuki T, Dohmae N and Simizu S: Identification of DPY19L3 as the *C*-mannosyltransferase of R-spondin1 in human cells. Mol Biol Cell 27: 744-756, 2016.
31. Perez-Vilar J, Randell SH and Boucher RC: C-Mannosylation of MUC5AC and MUC5B Cys subdomains. Glycobiology 14: 325-337, 2004.
32. Ihara Y, Manabe S, Ikezaki M, Inai Y, Matsui ISL, Ohta Y, Muroi E and Ito Y: *C*-Mannosylated peptides derived from the thrombospondin type 1 repeat interact with Hsc70 to modulate its signaling in RAW264.7 cells. Glycobiology 20: 1298-1310, 2010.
33. Buettner FF, Ashikov A, Tiemann B, Lehle L and Bakker H: *C. elegans* DPY-19 is a *C*-mannosyltransferase glycosylating thrombospondin repeats. Mol Cell 50: 295-302, 2013.
34. Shcherbakova A, Tiemann B, Buettner FFR and Bakker H: Distinct *C*-mannosylation of netrin receptor thrombospondin type 1 repeats by mammalian DPY19L1 and DPY19L3. Proc Natl Acad Sci USA 114: 2574-2579, 2017.
35. Fujiwara M, Kato S, Niwa Y, Suzuki T, Tsuchiya M, Sasazawa Y, Dohmae N and Simizu S: *C*-mannosylation of R-spondin3 regulates its secretion and activity of Wnt/β-catenin signaling in cells. FEBS Lett 590: 2639-2649, 2016.
36. Dong X, Liao W, Zhang L, Tu X, Hu J, Chen T, Dai X, Xiong Y, Liang W, Ding C, *et al*: RSPO2 suppresses colorectal cancer metastasis by counteracting the Wnt5a/Fzd7-driven noncanonical Wnt pathway. Cancer Lett 402: 153-165, 2017.
37. Tsuchiya M, Niwa Y and Simizu S: *N*-glycosylation of R-spondin1 at Asn137 negatively regulates its secretion and Wnt/β-catenin signaling-enhancing activity. Oncol Lett 11: 3279-3286, 2016.
38. Miyazaki S, Sasazawa Y, Mogi T, Suzuki T, Yoshida K, Dohmae N, Takao K and Simizu S: Identification of seco-clavilactone B as a small-molecule actin polymerization inhibitor. FEBS Lett 590: 1163-1173, 2016.
39. Miyazaki I, Simizu S, Ichimiya H, Kawatani M and Osada H: Robust and systematic drug screening method using chemical arrays and the protein library: Identification of novel inhibitors of carbonic anhydrase II. Biosci Biotechnol Biochem 72: 2739-2749, 2008.
40. Kawahara R, Niwa Y and Simizu S: Integrin β1 is an essential factor in vasculogenic mimicry of human cancer cells. Cancer Sci 109: 2490-2496, 2018.
41. Niwa Y, Suzuki T, Dohmae N and Simizu S: *O*-Fucosylation of CCN1 is required for its secretion. FEBS Lett 589: 3287-3293, 2015.
42. Yasukagawa T, Niwa Y, Simizu S and Umezawa K: Suppression of cellular invasion by glybenclamide through inhibited secretion of platelet-derived growth factor in ovarian clear cell carcinoma ES-2 cells. FEBS Lett 586: 1504-1509, 2012.
43. Simizu S, Umezawa K, Takada M, Arber N and Imoto M: Induction of hydrogen peroxide production and Bax expression by caspase-3(-like) proteases in tyrosine kinase inhibitor-induced apoptosis in human small cell lung carcinoma cells. Exp Cell Res 238: 197-203, 1998.
44. Matsuki W, Miyazaki S, Yoshida K, Ogura A, Sasazawa Y, Takao KI and Simizu S: Synthesis and evaluation of biological activities of vibsanin A analogs. Bioorg Med Chem Lett 27: 4536-4539, 2017.
45. Veeman MT, Slusarski DC, Kaykas A, Louie SH and Moon RT: Zebrafish prickle, a modulator of noncanonical Wnt/Fz signaling, regulates gastrulation movements. Curr Biol 13: 680-685, 2003.
46. Willert K, Brown JD, Danenberg E, Duncan AW, Weissman IL, Reya T, Yates JR III and Nusse R: Wnt proteins are lipid-modified and can act as stem cell growth factors. Nature 423: 448-452, 2003.
47. Komai K, Niwa Y, Sasazawa Y and Simizu S: Pirin regulates epithelial to mesenchymal transition independently of Bcl3-Slug signaling. FEBS Lett 589: 738-743, 2015.
48. Ishida K, Wierzba MK, Teruya T, Simizu S and Osada H: Novel heparan sulfate mimetic compounds as antitumor agents. Chem Biol 11: 367-377, 2004.
49. Nam JS, Turcotte TJ, Smith PF, Choi S and Yoon JK: Mouse cristin/R-spondin family proteins are novel ligands for the Frizzled 8 and LRP6 receptors and activate β-catenin-dependent gene expression. J Biol Chem 281: 13247-13257, 2006.
50. Hirschberg K, Miller CM, Ellenberg J, Presley JF, Siggia ED, Phair RD and Lippincott-Schwartz J: Kinetic analysis of secretory protein traffic and characterization of golgi to plasma membrane transport intermediates in living cells. J Cell Biol 143: 1485-1503, 1998.

51. Komekado H, Yamamoto H, Chiba T and Kikuchi A: Glycosylation and palmitoylation of Wnt-3a are coupled to produce an active form of Wnt-3a. Genes Cells 12: 521-534, 2007.
52. Hendee K, Wang LW, Reis LM, Rice GM, Apte SS and Semina EV: Identification and functional analysis of an *ADAMTSL1* variant associated with a complex phenotype including congenital glaucoma, craniofacial, and other systemic features in a three-generation human pedigree. Hum Mutat 38: 1485-1490, 2017.
53. Wang LW, Leonhard-Melief C, Haltiwanger RS and Apte SS: Post-translational modification of thrombospondin type-1 repeats in ADAMTS-like 1/punctin-1 by C-mannosylation of tryptophan. J Biol Chem 284: 30004-30015, 2009.
54. Li JS, Cui L, Rock DL and Li J: Novel glycosidic linkage in *Aedes aegypti* chorion peroxidase: *N-mannosyl tryptophan*. J Biol Chem 280: 38513-38521, 2005.
55. Brunner F, Wirtz W, Rose JKC, Darvill AG, Govers F, Scheel D and Nürnberger T: A β-glucosidase/xylosidase from the phytopathogenic oomycete, *Phytophthora infestans*. Phytochemistry 59: 689-696, 2002.
56. Moremen KW, Tiemeyer M and Nairn AV: Vertebrate protein glycosylation: Diversity, synthesis and function. Nat Rev Mol Cell Biol 13: 448-462, 2012.
57. Doucey MA, Hess D, Cacan R and Hofsteenge J: Protein C-mannosylation is enzyme-catalysed and uses dolichyl-phosphate-mannose as a precursor. Mol Biol Cell 9: 291-300, 1998.
58. Anand M, Rush JS, Ray S, Doucey MA, Weik J, Ware FE, Hofsteenge J, Waechter CJ and Lehrman MA: Requirement of the Lec35 gene for all known classes of monosaccharide-P-dolichol-dependent glycosyltransferase reactions in mammals. Mol Biol Cell 12: 487-501, 2001.